Battery Electrodes

DOI: 10.1002/anie.201410572

Wet-Chemical Synthesis of Phase-Pure FeOF Nanorods as High-Capacity Cathodes for Sodium-Ion Batteries**

*Jian Zhu and Da Deng**

Abstract: *It is challenging to prepare phase-pure FeOF by wet-chemical methods. Furthermore, nanostructured FeOF has never been reported. In this study, hierarchical FeOF nanorods were synthesized through a facile, one-step, wet-chemical method by the use of just $FeF_3{\cdot}3H_2O$ and an alcohol. It was possible to significantly control the FeOF nanostructure by the selection of alcohols with an appropriate molecular structure. A mechanism for the formation of the nanorods is proposed. An impressive high specific capacity of approximately 250 $mAh\,g^{-1}$ and excellent cycling and rate performances were demonstrated for sodium storage. The hierarchical FeOF nanorods are promising high-capacity cathodes for SIBs.*

Sodium-ion batteries (SIBs) have been attracting much attention in recent years as alternatives to the predominantly employed lithium-ion batteries (LIBs) for energy storage. There is increasing concern about the depletion of Li reserves located mainly in South America and the high cost of LIBs.[1] Expensive LIBs may not meet the increasing demand for large-scale applications, such as the mass adoption of electric vehicles and energy storage for renewable but intermittent solar and wind energy in smart grids. In contrast, Na reserves are abundant. Arguably, SIBs could be much cheaper than LIBs with comparable energy density.[1d] However, there is still a lack of suitable electrodes for SIBs. Owing to the larger radius of the Na ion ($r = 1.02$ Å) as compared to the Li ion ($r = 0.59$ Å) and their different ionic coordination properties, sodium ions have much slower solid-state diffusion kinetics, and the reaction kinetics of sodium-insertion/extraction reactions are much poorer than those of lithium ions.[1a,c,2] Therefore, nanoscale electrode materials should be employed to overcome these issues in the development of SIBs. At the same time, in the selection of electrodes for SIBs, attention must be paid to the differences and similarities of SIBs to LIBs. The conversion-type mixed-anion cathode material iron oxyfluoride (FeO_xF_{2-x}) is a promising cathode candidate for SIBs, although it has mainly been investigated for LIBs previously.[3] FeO_xF_{2-x} offers the combined advantages of fluorides, with a high reaction potential and high output voltages, and the beneficial effects of oxides, with improved capacity, conductivity, and cycling stability. The covalent Fe–O bonds in the highly ionic fluoride structure can improve electronic conductivity.[3a,4] FeOF ($x = 1$) has a theoretical capacity of 885 $mAh\,g^{-1}$,[5] which is larger than that of FeF_2 ($x = 0$; 571 $mAh\,g^{-1}$) and FeF_3 (712 $mAh\,g^{-1}$), assuming it is fully converted: $FeOF + 3\,Li \rightarrow Fe^0 + LiF + Li_2O$.[3a] Practically, the capacity should be much lower than the theoretical value owing to less than $3\,e^-$ transfer. Although FeOF has been investigated as a cathode candidate for LIBs, there is a lack of detailed studies on the electrochemical performance of nanostructured FeOF for applications in SIBs.[6]

The fabrication of electrode materials at the nanoscale is a generally accepted strategy to improve electrochemical performance in terms of cyclability, capacity, and charging rate.[7] However, high-capacity cathodes of FeOF with unique nanostructures (e.g. 1D nanorods) have not been reported so far to the best of our knowledge. It is very challenging to synthesize phase-pure FeOF nanostructures under mild conditions. In fact, the preparation of bulk FeOF even without any nanostructure is difficult. Typically, expensive experimental instruments and rigorous procedures must be used. For example, a solid-state reaction between Fe_2O_3 and FeF_3 as starting materials at a reaction temperature of about 950 °C has typically been used to prepare FeOF.[3b,6,8] However, this conventional method not only requires a high energy input and expensive sealed Pt tubes, but it is also difficult to obtain a pure single phase or nanostructured FeOF. Recently, much effort has been devoted to the development of alternative methods for the preparation of FeOF. The reaction between metallic Fe and H_2SiF_6 with subsequent heat treatment in air,[3a] the reaction of metallic Fe and dangerous HF acid,[4,5] and the fluorination of Fe_3O_4 in F_2 with heating[9] have been explored. The existing methods suffer from a number of notable limitations, such as the requirement of an ultrahigh temperature, expensive instruments, complex procedures, and the usage of highly corrosive HF and toxic F_2, and the difficulty in obtaining pure FeOF stoichiometry. Furthermore, no unique nanostructured FeOF could be formed by the reported methods.

Herein, we report the design and facile preparation of phase-pure hierarchical FeOF nanorods by a mild wet-chemical procedure with commercial $FeF_3{\cdot}3H_2O$ and an alcohol as the only reactant and solvent (see the Experimental Section). More importantly, we found that the nanostructures could be readily tuned by the selection of different alcohols; our observations helped us to understand the mechanism of formation of the FeOF nanorods. The as-prepared hierarchical FeOF nanorods were tested as cathode materials for SIB at ambient temperature, and very stable cycling performance was observed. An impressive specific capacity of approx-

[*] J. Zhu, Dr. D. Deng
Department of Chemical Engineering and Materials Science
Wayne State University
5050 Anthony Wayne Drive, Detroit, MI 48202 (USA)
E-mail: da.deng@wayne.edu

[**] We thank the Lumigen Instrument Center, Wayne State University.
Supporting information for this article is available on the WWW under http://dx.doi.org/10.1002/anie.201410572.

imately 250 mAh g^{-1} was reached without notable capacity fading, and good rate performance was demonstrated. The excellent electrochemical performance suggests that the as-prepared hierarchical FeOF nanorods are promising cathodes for future low-cost SIBs.

The phase purity of the hierarchical FeOF nanorods obtained with 1-propanol was evidenced by X-ray diffraction (XRD; Figure 1). All the peaks could be assigned to FeOF (JCPDS card no. 70-1522), and no impurity peaks were

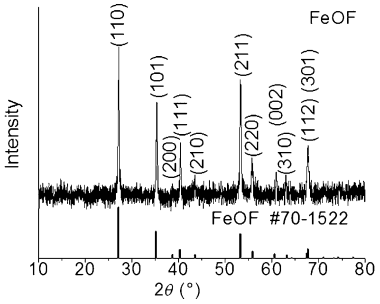

Figure 1. XRD pattern of as-prepared hierarchical FeOF nanorods.

observed. This XRD result suggests the successful and complete conversion of the precursors into FeOF. In other words, all the $FeF_3{\cdot}3H_2O$ was converted into hierarchical FeOF nanorods. The results of energy-dispersive X-ray spectroscopy (EDS) and its elemental mapping (see Figure S1 in the Supporting Information) further confirmed the formation of phase-pure FeOF. Another indication of complete conversion is that the solvent after the reaction was colorless; if Fe^{3+} ions were present in the solution, the typical yellow color of Fe^{3+} ions would be observed.

The morphology of the as-prepared hierarchical FeOF nanorods was thoroughly characterized by SEM and TEM (Figure 2). Only nanorods and rod assemblies (no other types of nanoparticles) were observed in the low-magnification overall view (Figure 2a), which indicates that the product was not only phase-pure by XRD but that its morphology was also highly identical. The as-prepared FeOF nanorods and assemblies had a totally different morphology to that of their precursor, irregular-shaped $FeF_3{\cdot}3H_2O$ (see Figure S2b), whose XRD pattern (see Figure S1a) was also totally different. Nanorod assemblies with different numbers of nanorods are apparent in Figure 2b. Generally, the assemblies have a 2D starlike structure when the number of nanorods is not more than six. Assemblies with more than six branches in the 3D structure are observed as well. The hierarchical nanorods are shown in more detail in Figure 2c. The rods in a six-nanorod assembly (Figure 2c, marked by ⑥) have a rod diameter of about 20–35 nm. The universal formation of hierarchical FeOF nanorods was also demonstrated by low-magnification TEM (Figure 2d). The inset in Figure 2d shows the selected-area electron diffraction (SAED) of the hierarchical FeOF nanorods. All the diffraction spots can be assigned to crystalline FeOF, thus indicating that the rods are single-crystalline. The detailed structures of a few representative multirod assemblies are shown in Figure 2e. High-

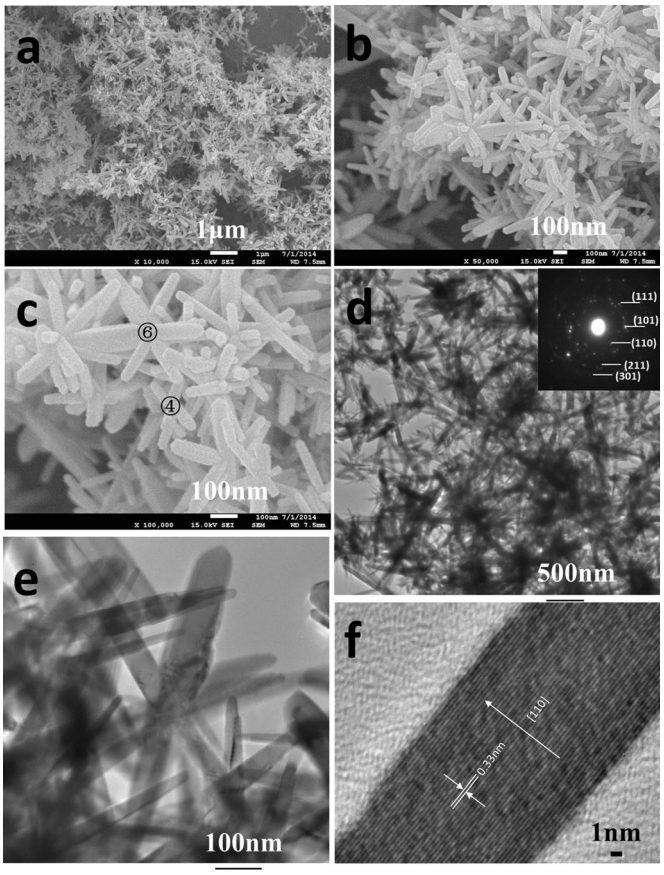

Figure 2. Field-emission SEM (FESEM) and TEM characterization of hierarchical FeOF nanorods. a) Low-magnification FESEM image showing that all structures formed are rods or starlike rod assemblies. b) Magnified FESEM image showing nanorod assemblies with different numbers of nanorods as branches. c) Magnified FESEM image showing the details of FeOF nanorod assemblies; the numbers in the circles indicate the number of rods in each assembly. d) Low-magnification TEM image of the structures. The inset is the selected-area electron diffraction (SAED) pattern of the FeOF nanorods. e) Magnified TEM image showing the details of hierarchical FeOF nanorods. f) HRTEM image of a section of a nanorod.

resolution (HR) TEM of a section of a single nanorod clearly showed that the nanorod was single-crystalline with a *d* space of 0.33 nm that can be assigned to the distance between (110) planes (Figure 2f). The nanorods grow in the [001] direction. The Fe atom in FeOF is in an octahedral environment, in which O and F occupy the opposite corners of an octahedron.[8] The average Fe–O and Fe–F bond lengths are 1.93 and 2.12 Å, respectively.[8] The lowest-energy FeOF structure ($P4_2/m(84)$) in the range of $3\times3\times2$ cells with projection along [001], [010], [100], and [111] directions is shown in Figure S3 of the Supporting Information.[8] The largest channels along the [001] direction are composed solely of O atoms, solely of F atoms, or of 50% O and 50% F atoms (see Figure S3a). Thus, the alignment of the channels along the growth direction of the nanorods was experimentally evidenced by HRTEM.

To understand the mechanism of formation of the hierarchical FeOF nanorods, we used five additional alcohols,

namely, methanol (CH_3OH), ethanol (CH_3CH_2OH), 1-pentanol ($CH_3CH_2CH_2CH_2CH_2OH$), 2-propanol ($CH_3CHOHCH_3$), and ethylene glycol ($HOCH_2CH_2OH$), as solvents instead of 1-propanol ($CH_3CH_2CH_2OH$). The products obtained were investigated thoroughly. Rodlike structures formed not only in 1-propanol, but also in the other three straight-chain monohydric alcohols tested: methanol, ethanol, and 1-pentanol (Figure 3a–c). FeF_3 nanorods with a larger diameter and a hexagonal cross-section formed in methanol (Figure 3a). The morphology of FeOF prepared in pure ethanol was similar to that of FeOF obtained with 1-propanol (Figure 3b). Nanorod assemblies were also observed when 1-pentanol was used as the only solvent. However, some nanoparticles were formed as a by-product (Figure 3c). Interestingly, no rodlike structures were observed for samples prepared in the branched-chain monohydric alcohol 2-propanol (Figure 3d) or the dihydric alcohol ethylene glycol (Figure 3e). Only nanoparticle aggregates and irregular microparticles were formed with 2-propanol and ethylene glycol, respectively.

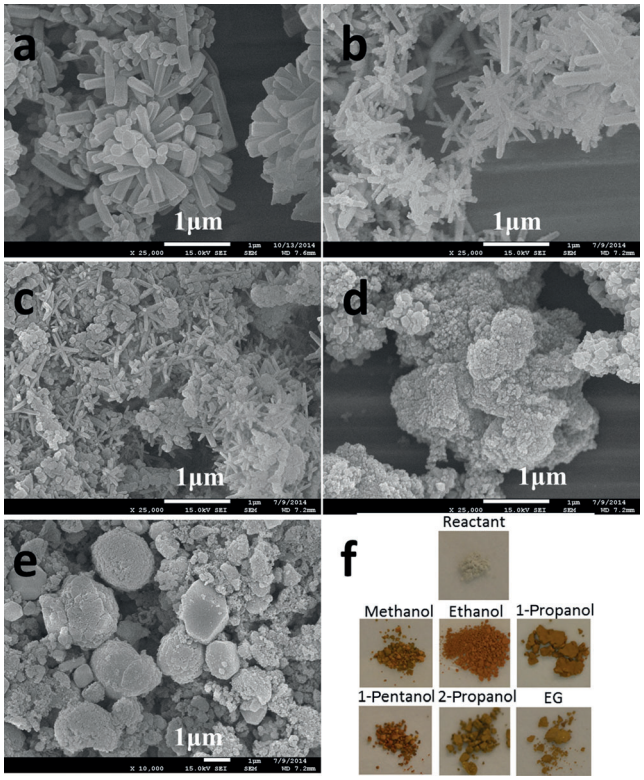

Figure 3. Effect of different alcohols on the structures. a–e) FESEM images of samples prepared in: a) methanol, b) ethanol, c) 1-pentanol, d) 2-propanol, and e) ethylene glycol (EG). f) Optical image of the precursor $FeF_3{\cdot}3\,H_2O$ and solid samples obtained in different alcohols.

As a 3d transition metal, iron can bind with ligands to form a coordination complex.[10] The $FeF_3{\cdot}3\,H_2O$ might undergo dehydration in the non-aqueous system of an alcohol R-OH, which may play a dual role as both the solvent and a binding ligand.[11] The binding of Fe and the ligand $-OR$ to form a Fe–OR bond may play a critical role in tuning the growth and formation of the nanostructures. The $RO-$ ligands could be seen to function as the facet-controlling agents by significantly affecting the surface energy during the growth of nanostructures, thus leading to anisotropic crystal growth.[12] Additionally, the length of the carbon chains of the ligands can significantly affect the binding ability and surface energy. Monohydric alcohols ROH with $R = CH_3$, CH_3CH_2, or $CH_3CH_2CH_2$ led to the formation of nanorod assemblies. The alcohol with $R = CH_3CH_2CH_2CH_2CH_2$ led to the formation of both nanorods and nanoparticles. This observation suggests that it is more difficult for $CH_3CH_2CH_2CH_2CH_2O-$ with a longer alkyl group to bind with iron atoms than it is for the ligands CH_3O-, CH_3CH_2O-, and $CH_3CH_2CH_2O-$ with shorter alkyl groups, probably as a result of steric hindrance.[13] When the solvent was changed from 1-propanol to 2-propanol, no rodlike structures were observed (Figure 3d). This observation indicates the different binding capability of 1-propanol and 2-propanol owing to a different arrangement of the nonpolar alkyl groups and the location of the hydroxy group. When the dihydric alcohol ethylene glycol was used, no nanorods were formed either, and the particle-size distribution was poor. This result suggests that dihydric alcohols with two symmetrical polar hydroxy groups are not good facet-controlling agents, possibly because one dihydric alkoxide (OCH_2CH_2O) tends to bind to two iron atoms at the same time, thus leading to the formation of large particles, that is, with microscale instead of nanoscale dimensions (Figure 3e). The color change from pale to brown was observed for all samples synthesized in different alcohols (Figure 3f), thus indicating the successful transformation of $FeF_3{\cdot}3\,H_2O$, and the synthesis is highly scalable. The composition was characterized by XRD to be FeF_3 in the case of methanol, FeOF in the case of ethanol/1-propanol, and "XRD amorphous" for the other tested alcohols.

We propose a possible mechanism for the formation of FeOF in the pure alcohol system. As a typical transition metal, the Fe atom can bind with $-F$, $-OR$, or $-OH$; therefore, the intermediate $FeF_x(OH)_y(OR)_{3-x-y}$ could be formed in the given reaction environment. Possible representative dehydration, alcoholysis, hydrolysis, and dealcoholysis reactions involved in the formation of phase-pure FeOF could be:[14]

$$FeF_3 \cdot 3\,H_2O \rightarrow FeF_3 + 3\,H_2O \quad (1)$$

$$FeF_3 + x\,HOR \rightarrow FeF_{3-x}(OR)_x + x\,HF \quad (2)$$

$$FeF_{3-x}(OR)_x + (2-x)\,H_2O \rightarrow FeF(OR)_x(OH)_{2-x} + (2-x)\,HF \quad (3)$$

$$FeF(OR)_x(OH)_{2-x} \rightarrow FeOF + x\,HOR + (1-x)\,H_2O \quad (4)$$

In our reaction systems, the amount of Fe, F, and H_2O present is fixed by the precursor $FeF_3{\cdot}3\,H_2O$, and the alcohols/alkoxides are abundant. The alkoxides may function as the facet-controlling agents to assist the formation of FeOF naorods. The alkoxides OR with $R = CH_3CH_2$, $CH_3CH_2CH_2$, and $CH_3CH_2CH_2CH_2CH_2$, may prefer to be the terminal groups attached to (110) facets to achieve the lowest surface energy, thus leading to the growth of the nanorods in the [001] direction. On the other hand, in the case of 2-propanol and

ethylene glycol, the corresponding alkoxides offer different surface-binding or coordination preferences as compared to those of the straight-chain alkoxides, thus leading to the formation of particles instead. This hypothesis is also supported by our observation that the nature of the alcohol has great impact on the morphology/composition of the final product.

A nanorod-splitting phenomenon was observed (see Figures S5–S9). The diameter of each subrod was smaller than that of the unsplit mother rod. In TEM images of nanorod assemblies with different numbers of branches (see Figure S8), cavities were observed at the joints of rods in all assemblies. These cavities which might be formed by the mechanical deformation/breakdown caused by rod splitting and the reoriented alignment of the rods in the assembly.[15] The TEM images (see Figure S8) revealed the formation of nanorod branches with different diameters/lengths as hierarchical structures with 3, 4, 6, and 12 nanorods. The observations suggest that the formation of sub-nanorods may start from the splitting of mother rods on the basis of a combined crystal-splitting mechanism[15,16] and an oriented attachment/assembly process.[17] The splitting mechanism could be similar to that of Bi_2S_3, which can form 2D tri-, tetra-, and hexapod structures. The fast crystal growth in the oversaturated solution provide the right conditions for splitting.[16a] However, the exact mechanism for the formation of hierarchical FeOF nanorods still requires further investigation, which we are pursuing with the assistance of computational modeling.

The electrochemical performance of the as-prepared hierarchical FeOF nanorods was evaluated (Figure 4). Our analysis herein is derived from our understanding of LIBs.[3–5] The first two cycles of the charge–discharge profile are shown in Figure 4a. The open-circuit voltage is about 2.20 V. In analogy to LIBs, the first discharge (sodiation) slope, from about 1.75 V to about 1.25 V with a plateau, could be associated with the insertion of Na ions into FeOF [Eq. (5)]; and the plateau at approximately 1.0 V might be attributed to the partial formation of NaF, Na_2O, and metallic Fe [Eq. (6)].[3–5]

$$Fe^{3+}OF + Na \rightarrow NaFe^{2+}OF \quad (5)$$

$$NaFe^{2+}OF + 2\,Na \rightarrow NaF + Na_2O + Fe^{0} \quad (6)$$

In the second sodiation process, no distinguishable plateaus can be observed, and a slope from about 3.0 to 1.0 V can be observed. To better interpret the results, we analyzed the dQ/dV plot similarly (see Figure S10). The cycling performance at 10 mA g^{-1} shows that the specific capacity can be maintained at about 250 mAh g^{-1} for 20 cycles (Figure 4b). Furthermore, the specific capacity can be maintained at about 210 mAh g^{-1} for another 20 cycles at a doubled rate of 20 mA g^{-1}. The good cycling performance of FeOF nanorods suggests that the nanostructured FeOF offers better electrode cyclability than random particles.[6]

In summary, we have successfully prepared hierarchical FeOF nanorods through a novel and facile alcohol-assisted solvothermal method. The method could be expanded to the synthesis of other mixed-anion materials ($M_xA_{1y}A_{2z}$). The molecular structure of the alcohols, including the alkyl-chain length, the alkyl-chain arrangement, and the location and number of hydroxy groups, can significantly control the composition/structure of the FeOF obtained. The as-prepared FeOF nanorod assembly shows excellent cycling and rate performance for SIBs at room temperature. These results suggest that the FeOF nanorods can be applied as high-capacity low-cost cathodes with excellent cyclability for SIBs.

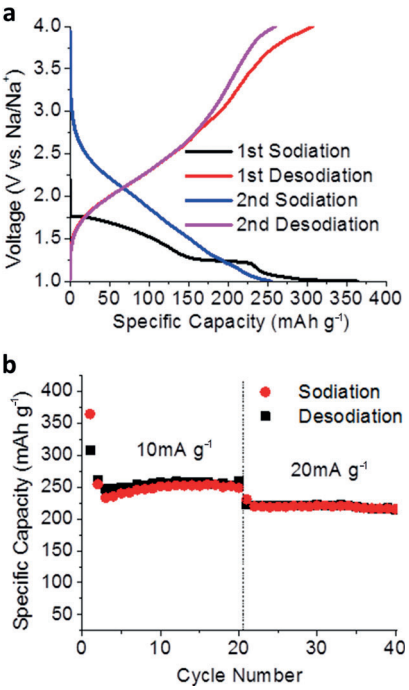

Figure 4. Electrochemical performance of the hierarchical FeOF nanorods as cathodes for SIBs. a) Charge–discharge profile of the first two cycles. b) Cycling and rate performance. Test conditions: currents of 10 and 20 mA g^{-1}; voltage window of 1–4 V.

Experimental Section

All the reagents used were of analytical grade from Sigma Aldrich (USA) and were used as received without purification. Typically, $FeF_3{\cdot}3H_2O$ (66.8 mg) was added to 1-propanol (32 mL) in a 45 mL Teflon reactor. The mixture was stirred for 5 min and then heated to 200 °C and maintained at this temperature for 24 h. The reactor was then allowed to cool down naturally under ambient conditions, and the as-prepared brown powder was washed with pure ethanol three times and dried in a vacuum at 50 °C overnight. For the study of solvents, other alcohols were used in place of 1-propanol, and all other conditions remained the same.

Received: October 29, 2014
Published online: January 21, 2015

Keywords: electrochemistry · iron oxyfluoride · nanorods · sodium-ion batteries · wet chemistry

[1] a) L. Xiao, Y. Cao, J. Xiao, W. Wang, L. Kovarik, Z. Nie, J. Liu, *Chem. Commun.* **2012**, *48*, 3321 – 3323; b) Y. Cao, L. Xiao, M. L. Sushko, W. Wang, B. Schwenzer, J. Xiao, Z. Nie, L. V. Saraf, Z.

Yang, J. Liu, *Nano Lett.* **2012**, *12*, 3783 – 3787; c) V. Palomares, P. Serras, I. Villaluenga, K. B. Hueso, J. Carretero-González, T. Rojo, *Energy Environ. Sci.* **2012**, *5*, 5884 – 5901; d) M. D. Slater, D. Kim, E. Lee, C. S. Johnson, *Adv. Funct. Mater.* **2013**, *23*, 947 – 958.

[2] a) Y. Fang, L. Xiao, J. Qian, X. Ai, H. Yang, Y. Cao, *Nano Lett.* **2014**, *14*, 3539 – 3543; b) P. W. D. P. J. Atkins, *Atkins' Physical Chemistry*, W. H. Freeman, New York, **2006**; c) Y. J. Zhu, Y. H. Xu, Y. H. Liu, C. Luo, C. S. Wang, *Nanoscale* **2013**, *5*, 780 – 787.

[3] a) N. Pereira, F. Badway, M. Wartelsky, S. Gunn, G. G. Amatucci, *J. Electrochem. Soc.* **2009**, *156*, A407 – A416; b) A. Kitajou, H. Komatsu, R. Nagano, S. Okada, *J. Power Sources* **2013**, *243*, 494 – 498.

[4] K. M. Wiaderek, O. J. Borkiewicz, E. Castillo-Martínez, R. Robert, N. Pereira, G. G. Amatucci, C. P. Grey, P. J. Chupas, K. W. Chapman, *J. Am. Chem. Soc.* **2013**, *135*, 4070 – 4078.

[5] M. Sina, K. W. Nam, D. Su, N. Pereira, X. Q. Yang, G. G. Amatucci, F. Cosandey, *J. Mater. Chem. A* **2013**, *1*, 11629 – 11640.

[6] S. Okada in 224th ECS Meeting (October 27 – November 1, 2013), Ecs, **2013**.

[7] a) X. Su, Q. Wu, J. Li, X. Xiao, A. Lott, W. Lu, B. W. Sheldon, J. Wu, *Adv. Energy Mater.* **2014**, *4*, 1300882; b) Y. Wu, Y. Wei, J. Wang, K. Jiang, S. Fan, *Nano Lett.* **2013**, *13*, 818 – 823; c) Y. Li, J. Yao, E. Uchaker, J. Yang, Y. Huang, M. Zhang, G. Cao, *Adv. Energy Mater.* **2013**, *3*, 1171 – 1175.

[8] V. L. Chevrier, G. Hautier, S. P. Ong, R. E. Doe, G. Ceder, *Phys. Rev. B* **2013**, *87*, 094118.

[9] H. Zhou, J. Nanda, S. K. Martha, J. Adcock, J. C. Idrobo, L. Baggetto, G. M. Veith, S. Dai, S. Pannala, N. J. Dudney, *J. Phys. Chem. Lett.* **2013**, *4*, 3798 – 3805.

[10] a) L. S. Zhong, J. S. Hu, H. P. Liang, A. M. Cao, W. G. Song, L. J. Wan, *Adv. Mater.* **2006**, *18*, 2426 – 2431; b) S. Jin, H. Deng, D. Long, X. Liu, L. Zhan, X. Liang, W. Qiao, L. Ling, *J. Power Sources* **2011**, *196*, 3887 – 3893.

[11] C. Li, L. Gu, S. Tsukimoto, P. A. van Aken, J. Maier, *Adv. Mater.* **2010**, *22*, 3650 – 3654.

[12] H. G. Yang, C. H. Sun, S. Z. Qiao, J. Zou, G. Liu, S. C. Smith, H. M. Cheng, G. Q. Lu, *Nature* **2008**, *453*, 638 – U634.

[13] D. C. Bradley, *Chem. Rev.* **1989**, *89*, 1317 – 1322.

[14] a) E. Kemnitz, U. Groß, S. Rüdiger, C. S. Shekar, *Angew. Chem. Int. Ed.* **2003**, *42*, 4251 – 4254; *Angew. Chem.* **2003**, *115*, 4383 – 4386; b) S. Rüdiger, U. Groß, E. Kemnitz, *J. Fluorine Chem.* **2007**, *128*, 353 – 368; c) S. Rüdiger, E. Kemnitz, *Dalton Trans.* **2008**, 1117 – 1127; d) L. D. Carlo, D. E. Conte, E. Kemnitz, N. Pinna, *Chem. Commun.* **2014**, *50*, 460 – 462.

[15] S. I. Cha, K. H. Hwang, Y. H. Kim, M. J. Yun, S. H. Seo, Y. J. Shin, J. H. Moon, D. Y. Lee, *Nanoscale* **2013**, *5*, 753 – 758.

[16] a) J. Tang, A. P. Alivisatos, *Nano Lett.* **2006**, *6*, 2701 – 2706; b) H. Deng, C. Liu, S. Yang, S. Xiao, Z.-K. Zhou, Q.-Q. Wang, *Cryst. Growth Des.* **2008**, *8*, 4432 – 4439; c) Q. Liu, Y. Zhou, Z. Tian, X. Chen, J. Gao, Z. Zou, *J. Mater. Chem.* **2012**, *22*, 2033 – 2038.

[17] a) D. Zitoun, N. Pinna, N. Frolet, C. Belin, *J. Am. Chem. Soc.* **2005**, *127*, 15034 – 15035; b) X. Zhong, R. Xie, L. Sun, I. Lieberwirth, W. Knoll, *J. Phys. Chem. B* **2006**, *110*, 2 – 4.

